Biointerface Research in Applied Chemistry
Platinum Open Access Journal (ISSN: 2069-5837)

Article
Volume 11, Issue 6, 2021, 15058 - 15067
https://doi.org/10.33263/BRIAC116.1505815067

Synthesis of Calcium Phosphate Extracted from Eggshell Waste through Precipitation Method

Aisyah Razak [1], Najah Mat Isa [1], Sharifah Adzila [1,*]

[1] Faculty of Mechanical & Manufacturing Engineering, Universiti Tun Hussein Onn Malaysia (UTHM), Parit Raja, 86400, Malaysia
* Correspondence: adzila@uthm.edu.my (S.A.);

Scopus Author ID 43760889800
Received: 8.03.2021; Revised: 4.04.2021; Accepted: 6.04.2021; Published: 9.04.2021

Abstract: Biomaterials for bone engineering applications are eagerly developing as traditional bone grafting methods show several drawbacks after and during operation. Eggshell waste contains high calcium suitable for developing biomaterials in hard tissue engineering as bone made up of calcium and phosphate. The precipitation method is one of the synthesis methods to produce calcium phosphate (CaP). In this work, calcium source was extracted from eggshell waste while phosphate source was from ortho-phosphoric acid. The synthesized CaP powder was calcined at different temperatures. X-ray diffraction (XRD) analysis shows two types of CaP patterns are hydroxyapatite (HA) and β-Tricalcium phosphate (β-TCP). Fourier transform infrared (FTIR) shows phosphate ion band in every sample while scanning electron microscopy (SEM) shows the transformation of structure from needle-like to more fluffy and rounded-edge structure from uncalcined to 1000°C. From the results obtained, CaP extracted from eggshell waste was successfully synthesized from the precipitation method. This method contributes to the materials processing cost reduction and increases the application of natural materials instead of synthetic ones.

Keywords: Biomaterials; eggshell waste; calcium phosphate; hydroxyapatite

1. Introduction

Bone is a dynamic and highly vascularized tissue that exhibits the unique capacity to remodel and heal without leaving scars. It provides structural support for the body and acts as a mineral reservoir as well [1,2]. Besides, the bone is living tissue that is the hardest among other connective tissues in the body [3]. Bone comprises 50 to 70% mineral, 20 to 40% organic matrix, 5 to 10% water, and <3% lipids [4–6]. But, it does not mean bone cannot be injured or affected by diseases. Once a fracture or disease occurs on bone, bone grafting becomes the option of regenerating the bone. Bone graft is a surgical procedure to reconstruct bone after trauma, infection, or disease, improve bone healing response, and regenerate bone tissue around implanted devices [7–9]. The three main types of bone graft are autografts, allografts and xenografts. Autografts or autologous grafts are the gold standard in bone grafts as they contain both standards in bone grafts since it contains both osteogenic cells and an osteoconductive mineralized extracellular matrix where these can grow and proliferate. Autografts are harvested bone tissues from the same patient for transplanting to the place it is needed [10,11]. However, this type of graft's major drawback is a secondary surgical operation performed at the tissue harvest site that may result in complications such as donor side damage, defect, traumatize, and morbidity [10]. To overcome this problem, allografts being introduced.

Allografts are bones from a donor of the same species for bone graft procedure. Allograft provides an alternative option for the treatment of complicated bony defects. However, allografts lead to other problems, including the risk of infections, an immune response of host tissue, disease transmission, and limited biological and mechanical properties [12,13]. Then, a bone donor from different species being introduced, known as xenograft. Cruciate ligament from porcine and dog tibia being used for bone grafting process. However, due to high immunity, insufficient biomechanical qualities, and foreign body reaction, this type of bone graft is abandoned as it creates a new problem rather than developing a new solution from limitations in autograft and allograft [7,14]. From all the disadvantages of autografts, allografts and xenografts, biomaterials are introduced to overcome that issue.

Biomaterials is a systemically and pharmacologically inert substance designed for implantation within or incorporation with living systems [15,16]. In simple terms, biomaterials are any material, natural or human-made, consisting of a whole or part of a living structure or biomedical device that performs, enhances, or replaces a natural function [17]. Calcium phosphate (CaP) is one of the biomaterials that researchers eagerly develop due to its suitability to be used as a carrier for drugs, non-viral gene delivery, antigens, enzymes, and proteins [18,19]. Besides, CaP also an excellent material in bioactivity and biocompatibility [20]. Based on industry trends, the CaP market size value in 2018 was over USD 640 million and is expected to increase by over 5% in 2025 [21,22]. From this trend, CaP is still relevant to be produced due to its market demand. Three types of CaP show high research interest. These are hydroxyapatite (HA), tricalcium phosphate (TCP), and biphasic calcium phosphate (BCP). In bone engineering application, calcium phosphate from HA, TCP, and BCP becomes a choice as it calcium to phosphorus (Ca/P) ratio in the range of bone Ca/P ratio 1.37 to 1.87 [23,24]. To produce CaP, calcium and phosphate precursor must be mixed together through the precipitation process with an additional pH adjuster to make sure the solution in the alkaline pH range. Calcium precursors in this research work from chicken eggshell waste converted to calcium oxide (CaO). Eggshell waste contains a high percentage of calcium contains (94-97%) in calcium carbonate ($CaCO_3$) or also known as calcite form [25,26]. To date, eggshells can serve as a promising biomaterials source because of their continuous resource compared to other natural sources of CaP like bovine bones and corals. Obtaining CaO is essential as it is a raw material for producing CaP that will be further synthesized through various synthesis methods such as precipitation, sol-gel, etc., in the manufacturing of scaffolds or any other biomedical needs [27–30].

This research work focused on the synthesis of CaP from chicken eggshells as the source of calcium precursor with phosphate precursor from ortho-phosphoric acid and additional ammonia solution that act as pH adjuster. The chemical, physical, and morphological properties of the materials were studied.

2. Materials and Methods

2.1. Sample preparation.

The collected eggshells were washed and immersed in boiling water for 30 minutes to remove any surface contaminants. Next, these eggshells were dried in the oven for 3 hours before crushed into smaller flakes using alumina mortar. Then, these eggshell flakes were calcined at a temperature of 900°C for 4 hours in the furnace for a complete transformation of $CaCO_3$ into CaO powders to ensure complete carbon dioxide removal (CO_2) [31].

2.2. Synthesis of CaP.

CaP powders were prepared by using the wet chemical precipitation method. CaO powders obtained were introduced into a beaker containing 250 ml of distilled water and stirred for 30 minutes at a temperature of 60°C. The powder was ultimately dissolved by warming the solution.

$$CaO + H_2O = Ca(OH)_2$$

Then, 14.7 ml of ortho-phosphoric acid (H_3PO_4) dissolved in 250 ml of distilled water were added into the suspension and continue to be stirred until temperature up to 80°C producing white-colored precipitate. Next, ammonia solution (NH_3) was added as a pH adjustment until the suspension's pH reached 9-12. The reacted suspension, which was milky, was left resting (aging) in the fume cupboard for 24 hours before the precipitation product was filtered.

$$3Ca(OH)_2 + 2H_3PO_4 \xrightarrow{NH_3} Ca_3(PO_4)_2 + 6H_2O$$

The solid white product collected from filtration was oven-dried at a temperature of 80°C for 2 hours. The product was then rinsed with distilled water and filtered again to dissolve any unreacted phosphate during the reaction process. Later, the product was oven-dried at a temperature of 100°C for 2 hours. The agglomerated white powder was crushed using a mortar and sieved until the size powder's average obtained was ≈ ≦60 µm. Lastly, the synthesized powder was calcined at various temperatures of 600, 700, 800, 900 and 1000°C for 3 hours at 5°C/min of heating and cooling rates. The calcined powder was roughly crushed in a mortar and pestle to get the final refine powder.

2.3. Characterization.

2.3.1. X-ray diffraction (XRD).

The phase analysis of calcined powders was determined under XRD analysis. All the uncalcined and calcined powders were placed into the sample holder. This instrument works with voltage and the current setting of 30 kV and 40 mA, respectively, and uses Cu-Kα radiation (λ=0.15406 nm). For qualitative analysis, XRD diagrams were recorded in 2θ=10°-100° at a step size of 0.02°, and the step time is 2s per step. Then, the lattice parameters and atomic position were refined by using OriginPro 2018 and X'Pert HighScore software programs.

2.3.2. Fourier transform-IR (FTIR).

The functional group of synthesized calcium phosphate powders was obtained using an FTIR spectrometer. All powder samples must be finely ground to reduce scattering losses and absorption band distortions. Attenuated Total Reflection (ATR) powder technique was used with range 600 to 4000 cm^{-1}; accommodation 32 scan and resolution of 4 cm^{-1}.

2.3.3. Scanning electron microscopy (SEM).

Morphological analysis of the powder samples was examined under SEM with high magnification, and EDX was performed to determine each sample's percentage composition. All samples were double-coated by gold using a sputter coater on the surface to create a conductive layer and reduce the samples' charging.

3. Results and Discussion

3.1. Characterization of CaP.

3.1.1. X-ray diffraction (XRD) analysis.

The identification of the crystalline phase of uncalcined and calcined CaP powders at a temperature range from 600 to 1000°C was conducted by X-ray diffraction to confirm the phase existence. The diffraction patterns are shown in Figure 1.

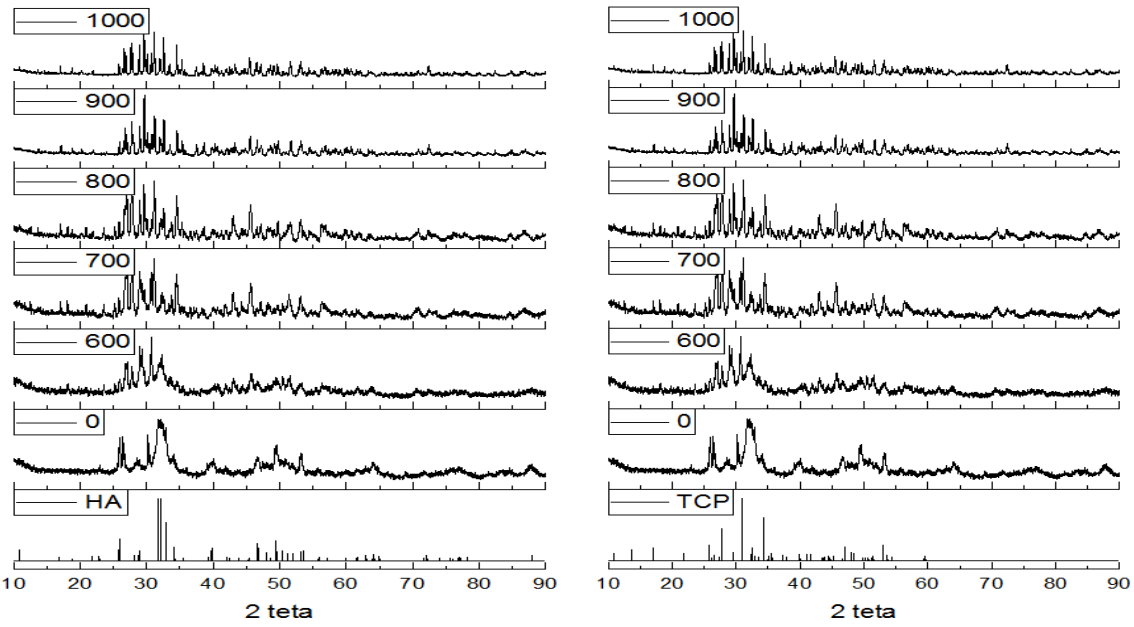

Figure 1. XRD pattern for a sample at different temperatures. (**a**) HA pattern; (**b**) TCP pattern.

The crystalline phase of HA powder confirmed the formation of an amorphous CaP precursor, as shown by significant peaks appear at (111), (002), (211), (112), (130), (213), (004), (323), (323), (210), (401), (313), (321) and (333) planes respectively in accordance to JCPDS file no. 74-0566. The characteristics of XRD patterns of hexagonal symmetry HA powder were identified at a temperature range from 0 to 700°C. The sharp peaks are obtained at 2θ value of 26°, 32°, 46°, 49°, 57°, and 64° indicates complete crystallization of the synthesized HA. Moreover, the broad peaks indicating low crystallinity of HA are obtained at 2θ values of 30°-35°, 49°-53°, and 64° as a result of impurity in synthesized HA powder. Besides, it is confirmed that there is no other crystalline phase, and there are no concurrences of secondary phases other than HA during HA formation. Furthermore, the HA's peaks were further reduced, indicating the gradual disappearance of HA and the appearance of β-TCP as a secondary phase. When heat-treated at 700°C, these peaks biphasic can be discovered where at 2θ value of 25°, 33°, and 46° for HA whereas β-TCP peaks started to appears at 28°, 32°, and 36°. The new peaks of β-TCP match the JCPDS file no. 70-2065 belongs to the rhombohedral symmetry. As the temperature increase from 700 to 1000°C, the appearance of β-TCP peaks getting more distinct at (122), (211), (0210), (300) and (220) planes, respectively.

According to previous works, the sharper peaks of higher calcination temperature results indicate the higher crystallinity structure obtained. Besides, the formation of β-TCP may arise due to multiple variables during the synthesis process, such as chemical impurity, the concentration of aqueous solutions, processing pH, including calcination temperature [32]. In

addition, the profile of synthesized HA and β-TCP was in agreement with the profile of the commercial calcium phosphates. The reaction at 600°C showed the formation of HA with no other phase also at 700°C, although there is a small quantity of β-TCP. At the temperature of 800°C, the synthesized powder showed that β-TCP is easily formed at the beginning of higher heat treatment and remains the main phase until temperature reaches 1000°C. Other related works found that the HA phase can stabilize up to 1300°C [33]. The duration of calcination, which is 3 hours, did not significantly affect the crystalline powder produced than calcination temperature, which plays a crucial role in this experiment. It implies that, heat treatment must be performed at a minimum temperature of 600°C, as stated by previous works, to ensure complete removal of any organic substances and residue from the experiment's synthesized part [30]. Plus, higher calcination temperature can promote to more stable crystal with higher intensity of final products.

3.1.2. Fourier transform-IR (FTIR) analysis.

Fourier transform infrared (FTIR) spectrometry was analyzed to determine the functional group of both simultaneously uncalcined and calcined CaP. Figure 2 shows the IR spectra of both uncalcined (0ºC) and calcined CaP from 600 to 1000ºC.

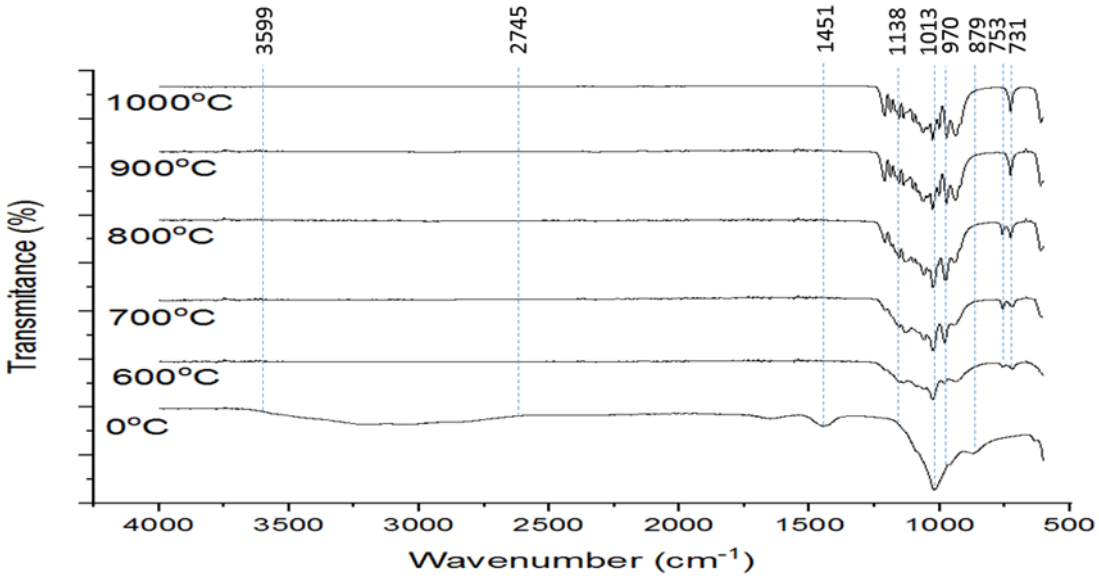

Figure 2. FTIR pattern of CaP powder at different temperatures.

Based on Figure 2, the FTIR pattern of uncalcined CaP shows broadband from 3599 to 2745 cm^{-1} indicates the presence of adsorbed water in the surface of the CaP particle due to moisture as the sample not being calcined [34,35]. From this broadband, it has been attributed as H-bonded water of humidity [36]. After CaP being calcined, this band disappears as heat removes water from the sample. Carbonate ion, CO_3^{-2}, bands were spot for temperature 0°C at 1451 and 879 cm^{-1} where it can be ascribed to B-type carbonate substitution on phosphate ion sites [37]. The presence of signals from the carbonate vibrations is typical of natural phosphates and can be associated with the phosphate groups' substitution by the carbonate ones inside the crystals [38]. Type B apatite has better bioactivity and is better for bone replacement due to its similarity to biological apatites in human bone [39]. For samples at temperatures 600 to 1000°C, CO_3^{-2} band does not appear. CO_3^{-2} is caused by an atmosphere-opened reaction that allows CO_2 incorporation into the particle's surface. After calcination, it is possible to observe a decrease in these bands' intensity because adsorbed groups tend to be eliminated at high

temperatures [34]. For phosphate ion PO_4^{-3} band, 1138 and 1013 cm^{-1} shows v_3 antisymmetric stretching while 970 cm^{-1} shows v_1 symmetric stretching [40,41]. v_2 symmetric bending and v_4 antisymmetric bending cannot be detected as the scanning range of this sample is 600 to 4000 cm^{-1} while v_2 and v_4 state around 599 to 460 cm^{-1}. However, the characteristic band position for the CaP band position can still be detected at 1138, 1013, and 970 cm^{-1}, which shows all this sample is in CaP form [38]. The band at 753 cm^{-1} indicates α-pyrophosphate, α- $P_2O_7^{-4}$ and when CaP being calcined to a temperature above 900°C this band disappears. The band at 731 cm^{-1} shows $P_2O_7^{-4}$ ion, where the intensity of this peak increase with the increasing calcination temperature. This peak becomes sharper by calcined the sample, which agrees with converting hydrogen phosphate ion, HPO_4^{-2} to β-TCP after calcination at 600 to 1000°C [42,43].

3.1.3. Scanning electron microscopy (SEM) analysis.

The morphological analyses of CaP powders were shown in Figure 3, which reveals the favorable outcome in the synthesis of CaP particles with an average 60µm particle size in this experimental work. Morphology samples that did not experience heat treatment (Figure 3a) reveal petals and needle-like shapes for the most part. It also tends to become a more fibrous cluster due to poor crystallization due to low calcination temperature.

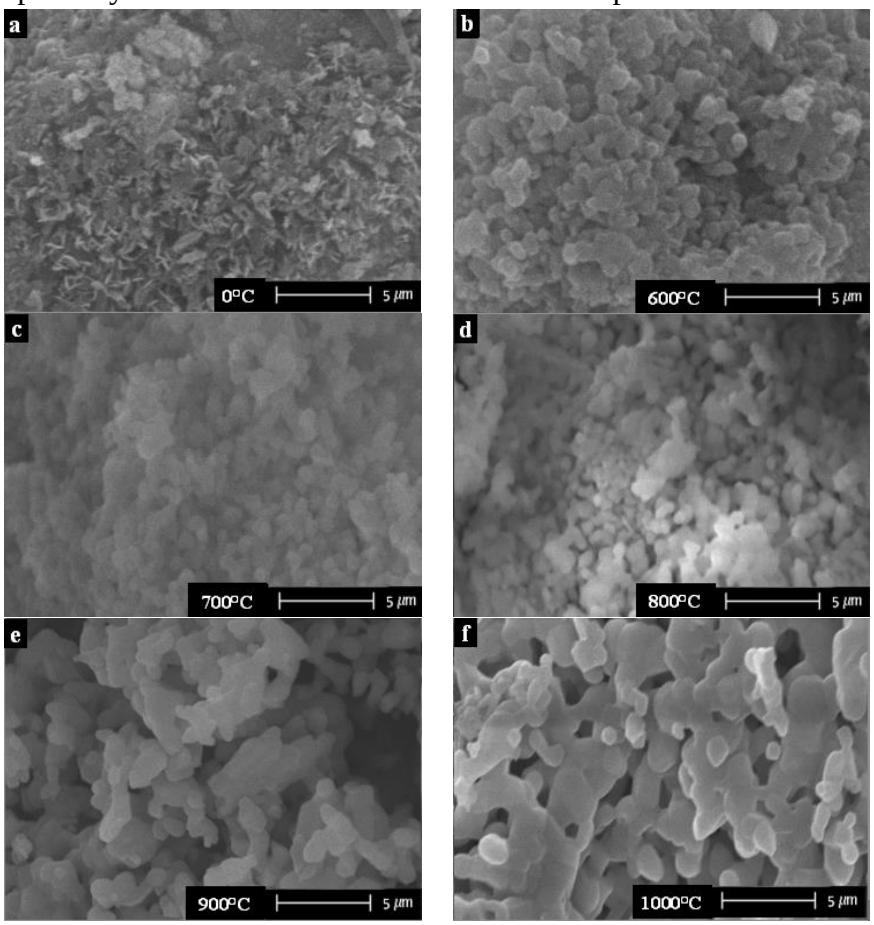

Figure 3. SEM image for CaP after calcined at different temperature: (**a**) 0°C; (**b**) 600°C; (**c**) 700°C; (**d**) 800°C; (**e**) 900°C; (**f**)1000°C.

Moving on to a temperature range of 600°C to 800°C (Figure 3b, c, d) showed the samples transform to more fluffy and rounded-edge, which is a typical morphological pattern for calcium phosphate powder that contains HA. Other related works also justify this pattern as a rice-like pattern that is formed by many agglomerations [27]. This emphasizes that morphology transformation is mainly due to the effect of high calcination temperature. As

mentioned, temperature affects crystal growth because of molecules' faster movement, resulting in them evaporating rapidly. Figure 3e responds to expectation where the agglomeration samples display irregular, more connected shapes starting to welded together. Pointed to the fact that at 1000°C, starting the formation of inter-particle necks and will grow along with the increase in temperature up to 1200°C, and the pore is starting to shrink [44].

Table 1. EDX analysis for CaP powder at different calcination temperatures.

Sample	Element	Atomic%	Weight%	Ca/P
0°C	Ca	61.96	67.83	1.63
	P	38.04	32.17	
600°C	Ca	60.58	66.53	1.54
	P	39.42	33.47	
700°C	Ca	59.70	65.72	1.48
	P	40.30	34.28	
800°C	Ca	57.14	63.42	1.36
	P	42.86	36.58	
900°C	Ca	54.79	61.07	1.21
	P	45.21	38.93	
1000°C	Ca	53.77	60.08	1.16
	P	46.23	39.92	

EDX analysis in Table 1 confirms the purity of the materials being composed solely of Ca and P and O and H. Even though the EDX analysis is qualitative. It can help identify the calcium and phosphorous ratio from the atomic percentage (atom %) [45]. The results of Ca/P ratio were calculated for all samples obtained, mainly calcium-deficient HA in which comparable to CaP found in bone and teeth. CaP with Ca/P ratio that is less than 1.5 would be likely less stable. This is because the higher Ca deficiency that leads to the imperfection of the structure [46]. The samples at temperature 600 and 1000°C display a Ca/P ratio <1.5, leading to the formation of β-TCP in which proved in XRD analysis where β-TCP starting to appear at 700°C. The presence of β-TCP in calcium phosphates powder can be benefited for its good solubility and degradation rate, which it can be chosen as starting materials for bioresorbable graft.

4. Conclusions

Calcium phosphate (CaP) is successfully synthesized through the precipitation process using eggshell waste treated with calcium oxide (CaO) as calcium precursor and ortho-phosphoric acid as phosphate precursor with additional ammonia solution that acts as pH adjuster. For XRD analysis, two types of CaP can be detected: hydroxyapatite (HA) and β-Tricalcium phosphate (β-TCP). FTIR analysis shows H- band, CO_3^{-2}, PO_4^{-3}, $P_2O_7^{-4}$ that occur due to different samples' calcination temperatures. SEM shows a needle-like shape for uncalcined CaP to more fluffy and rounded-edge for CaP calcined at 600 to 800°C, an irregular, more connected shape starting to weld together for sample 900°C and transform to inter-particle necks for 1000°C. Ca to P ratio (Ca/P) resulted in a 1.16 to 1.63 Ca/P ratio. The synthesized CaP powder with calcined CaP powder at 600 to 700°C suitable for biomedical implant in hard tissue engineering application based on its Ca/P ratio.

Funding

This research was funded by Post-Graduate Research Grant (GPPS), grant number H540 and Fundamental Research Grant Scheme (FRGS), grant number K199.

Acknowledgments

The authors wish to acknowledge their appreciation to the Faculty of Mechanical and Manufacturing Engineering (FKMP), Universiti Tun Hussein Onn Malaysia (UTHM), for the use of the facilities.

Conflicts of Interest

The authors declare no conflict of interest.

References

1. Lim, J.; You, M.; Li, J.; Li, Z. Emerging bone tissue engineering via polyhydroxyalkanoate (PHA) - Based scaffolds. *Mater. Sci. Eng. C* **2017**, *79*, 917–929, https://doi.org/10.1016/j.msec.2017.05.132.
2. Cao, G.; Huang, Y.; Li, K.; Fan, Y.; Xie, H.Q.; Li, X. Small intestinal submucosa: superiority, limitations and solutions, and potential to address bottlenecks in tissue repair. *J Mater Chem B* **2019**, *7*, 5038–5055, https://doi.org/10.1039/C9TB00530G.
3. Setiawati, R.; Rahardjo, P. Bone development and growth. In Osteogenesis and Bone Regeneration, 1st ed.; Yang, H., Eds.; IntechOpen: London, United Kingdom, **2019**; *1*, 1–20, https://doi:10.5772/intechopen.739554.
4. Von Euw, S.; Wang, Y.; Laurent, G.; Drouet, C.; Babonneau, F.; Nassif, N.; Azais, T. Bone mineral: New insights into its chemical composition. *Sci. Rep* **2019**, *9*, 1–11, https://doi.org/10.1038/s41598-019-44620-6.
5. Gasser, J.A.; Kneissel, M. Bone physiology and biology. In Bone Toxicology, 1st ed.; Smith, S.Y.; Varela, A.; Samadfam, R., Eds.; Springer: Cham, Switzerland, **2017**; *1*, 27–94, https://doi.org/10.1007/978-3-319-56192-9.
6. Adzila, S.; Mustaffa, N.A.; Kanasan, N. Magnesium-doped calcium phosphate/sodium alginate biocomposite for bone implant application. *J Aus Ceram Soc.* **2020**, *56*, 109–115, https://doi.org/10.1007/s41779-019-00417-4.
7. Dinçel, Y.M. Bone graft types. In Bone Grafting: Recent Advances with Special References to Cranio-Maxillofacial Surgery, 1st ed.; Kummoona R., Eds.; IntechOpen: London, United Kingdom, **2018**, *1*, 27–40, http://dx.doi.org/10.5772/intechopen.73956
8. Fillingham, Y.; Jacobs, J. Bone grafts and their substitutes. *Bone Jt. J.* **2016**, *98*, 6–9. https://doi.org/10.1302/0301-620X.98B.36350.
9. Li, R.; Zhu, G.; Chen, C.; Chen, Y.; Ren, G. Bone transport for treatment of traumatic composite tibial bone and soft tissue defects: any specific needs besides the Ilizarov Technique?. *BioMed Res. Int.* **2020**, *2020*, 1–13, https://doi.org/10.1155/2020/2716547.
10. Haugen, H.J.; Lyngstadaas, S.P.; Rossi, F.; Perale, G. Bone grafts: Which is the ideal biomaterial? *J. Clin. Periodontol.* **2019**, *46*, 92–102, https://doi.org/10.1111/jcpe.13058.
11. Baldwin, P.; Li, D.J.; Auston, D.A.; Mir, H.S.; Yoon, R.S.; Koval, K.J. Autograft, allograft, and bone graft substitutes: Clinical evidence and indications for use in the setting of orthopaedic trauma surgery. *J. Orthop. Trauma* **2019**, *33*, 203–213, https://doi.org/10.1097/BOT.0000000000001420.
12. Moore, M.A.; Samsell, B.; McLean, J. Allograft tissue safety and technology. In Biologics in Orthopaedic Surgery, 1st ed.; Wolfe, K.; Horigan, J., Eds.; Elsevier: Missouri, United States, **2019**; *1*, 49–62, https://doi.org/10.1016/B978-0-323-55140-3.00005-9.
13. Singh, H.; Moss, I.L. Chapter 15 - Biologics in spinal fusion. In Biologics in Orthopaedic Surgery, 1st ed., Mazzocca, A.D.; Lindsay, A.D., Eds.; Elsevier: Missouri, United States, **2019**; *1*, 165–174, https://doi.org/10.1016/B978-0-323-55140-3.00015-1.
14. Mahyudin, F.; Utomo, D.N.; Suroto, H.; Martanto, T.W.; Edward, M.; Gaol, I.L. Comparative effectiveness of bone grafting using xenograft freeze-dried cortical bovine, allograft freeze-dried cortical New Zealand white rabbit, xenograft hydroxyapatite bovine, and xenograft demineralized bone matrix bovine in bone defect of femoral diaphysis of white rabbit: Experimental study in vivo. *Int. J. Biomater* **2017**, *2017*, 1–9. https://doi.org/10.1155/2017/7571523.
15. Marin, E.; Boschetto, F.; Pezzotti, G. Biomaterials and biocompatibility: An historical overview. *J. Biomed. Mater. Res. A* **2020**, *108*, 1617–1633, https://doi.org/10.1002/jbm.a.36930.

16. Rezaie, H.R.; Rizi, H.B.; Khamseh, M.M.R.; Öchsner, A. Primary information about biomaterials. In A Review on Dental Materials, 1st ed., Rezaie, H.R.; Rizi, H.B.; Khamseh, M.M.R.; Öchsner, A., Eds.; Springer: Cham, Switzerland, **2020**; *1*, 1–30, https://doi.org/10.1007/978-3-030-48931-1_1.
17. Khan, M.Y.; Chen, M.H. A review on role of biomaterials in biomedical field. *IJBPR* **2019**, *8*, 2788–2793, https://doi.org/10.21746/ijbpr.2019.8.9.2.
18. Prokopowicz, M.; Szewczyk, A.; Skwira, A.; Sądej, R.; Walker, G. Biphasic composite of calcium phosphate-based mesoporous silica as a novel bone drug delivery system. *Drug Deliv. Transl. Res.* **2020**, *10*, 455–470, https://doi.org/10.1007/s13346-019-00686-3.
19. Levingstone, T.J.; Herbaj, S.; Dunne, N.J. Calcium phosphate nanoparticles for therapeutic applications in bone regeneration. *Nanomaterials* **2019**, *9*, 1570–1592, https://doi.org/10.3390/nano9111570.
20. Adzila, S.; Mustaffa, N.A.; Kanasan, N.; Nordin, N.; Rus, A.Z.M.; Bano, N. Effect of sodium alginate on the properties of calcium phosphate for bone implant application. *Int. J. Nanoelectron. Mater* **2020**, *13*, 1-9. https://ijneam.unimap.edu.my/images/PDF/InPress%20Special%20Issue%202020/Paper%20ID%204.pdf
21. Calcium Phosphate Market Outlook. Available online: https://www.gminsights.com/industry-analysis/calcium-phosphate-market (accessed on 13 September **2020**).
22. Calcium Phosphate Market 2019 to 2025: Global Industry Size, Share, Growth, Trends and Forecast. Available online: https://www.gminsights.com/industry-analysis/calcium-phosphate-market (accessed on 13 September 2020).
23. Sierra, L.A.Q.; Escobar, D.M. Characterization and bioactivity behavior of sol–gel derived bioactive vitroceramic from non-conventional precursors. *BOL SOC ESP CERAM V* **2019**, *58*, 85–92. https://doi.org/10.1016/j.bsecv.2018.07.003.
24. Campion, C.; Hing, K.A. Porous bone graft substitutes.In Mechanobiology Exploitation for Medical Benefit, 1st ed., Rawlinson, S.C., Eds., John Wiley & Sons: New Jersy, United Kingdom, **2017**; *1*, 347–371, https://doi.org/10.1002/9781118966174.ch21.
25. Owuamanam, S.; Cree, D. Progress of bio-calcium carbonate waste eggshell and seashell fillers in polymer composites: A review. *J. Compo. Sci.* **2020**, *4*, 70–92, https://doi.org/10.3390/jcs4020070.
26. Ajayan, N.; Shahanamol, K.P.; Arun, A.U.; Soman S. Quantitative variation in calcium carbonate content in shell of different chicken and duck varieties. *Advances in zoology and botany* **2020**, *8*, 1–5, https://doi.org/10.13189/azb.2020.080101.
27. Horta, M.; Aguilar, M.; Moura, F.; Campos, J.; Ramos, V.; Quizunda, A. Synthesis and characterization of green nanohydroxyapatite from hen eggshell by precipitation method. *Mater. Today* **2020**, *14*, 716–721. https://doi.org/10.1016/j.matpr.2019.02.011.
28. Hassanajili, S.; Pour, A.K.; Oryan A.; Khozani. T.T. Preparation and characterization of PLA/PCL/PHA composite scaffolds using indirect 3D printing for bone tissue engineering. *Mater. Sci. Eng. C.* **2019**, *104*, 1–13, https://doi.org/10.1016/j.msec.2019.109960.
29. Oladele, I.O.; Agbabiaka, O.G.; Adediran, A.A.; Akinwekomi, A.D.; Balogun, A.O. Structural performance of poultry eggshell derived hydroxyapatite based high density polyethylene bio-composites. *Heliyon* **2019**, *5*, 1–7. https://doi.org/10.1016/j.heliyon.2019.e02552.
30. Zaman, T.; Mostari, M.; Mahmood, M.A.A.; Rahman, M.S. Evolution and characterization of eggshell as a potential candidate of raw material. *Cerâmica* **2018**, *64*, 236–241, https://doi.org/10.1590/0366-69132018643702349.
31. Najah, M. I.; Razak, A.; Nekmat, N.A.C.S.; Adzila, S.; Othman, R.; Nordin, N. Characterization of calcium carbonate extracted from eggshell waste at various calcination temperature. *IJETER* **2020**, *8*, 6725–6731, https://doi.org/10.30534/ijeter/2020/168102020.
32. Pankaew, P.; Hoonnivath, E.; Limsuwan, P.; Naemchanth, K. Temperature effect on calcium phosphate synthesized from chicken eggshells and ammonium phosphate. *J. Appl. Sci.* **2010**, *10*, 3337–3342. https://doi.org/10.3923/jas.2010.3337.3342.
33. Ho, W.F.; Hsu, H.C.; Hsu, S.K.; Hung, C.W.; Wu, S.C. Calcium phosphate bioceramics synthesized from eggshell powders through solid state reaction. *Ceram. Int.* **2013**, *39*, 6467–6473. http://dx.doi.org/10.1016/j.ceramint.2013.01.076.
34. Caliman, L.B.; Silva, S.N.D.; Junkes, J.A.; Sagrillo, V.P.D. Ostrich eggshell as an alternative source of calcium ions for biomaterials synthesis. *Mater. Res.* **2017**, *20*, 413–417, https://doi.org/10.1590/1980-5373-mr-2016-0368.

35. Anjaneyulu, U.; Sasikumar, S. Bioactive nanocrystalline wollastonite synthesized by sol–gel combustion method by using eggshell waste as calcium source. *Bull. Mater. Sci.* **2014**, *37*, 207–212. https://doi.org/10.1007/s12034-014-0646-5.
36. Marques Correia, L.; Cecilia, J.A.; Rodríguez-Castellón, E.; Cavalcante, C.L.; Vieira, R.S. Relevance of the physicochemical properties of calcined quail eggshell (CaO) as a catalyst for biodiesel production. *J. Chem.* **2017**, *2017*, 1–12, https://doi.org/10.1155/2017/5679512.
37. Wu, S.C.; Hsu, H.C.; Hsu, S.K.; Chang, Y.C.; Ho, W.F. Synthesis of hydroxyapatite from eggshell powders through ball milling and heat treatment. *J. Asian Ceram. Soc.* **2016**, *4*, 85–90, https://doi.org/10.1016/j.jascer.2015.12.002.
38. Kalbarczyk, M.; Szcześ, A.; Sternik, D. The preparation of calcium phosphate adsorbent from natural calcium resource and its application for copper ion removal. *Environ. Sci. Pollut. Res.* **2021**, *28*, 1725–1733, https://doi.org/10.1007/s11356-020-10585-7.
39. Hamidi, A.A.; Salimi, M.N.; Yusoff, A.H.M. Synthesis and characterization of eggshell-derived hydroxyapatite via mechanochemical method: A comparative study. *AIP Conf. Proc.* **2017**, *1835*, 1–13, https://doi.org/10.1063/1.4981867.
40. Rau, J.V.; Wu, V.M.; Graziani, V.; Fadeeva, I.V.; Fomin, A.S.; Fosca, M.; Uskoković, V. The Bone Building Blues: Self-hardening copper-doped calcium phosphate cement and its in vitro assessment against mammalian cells and bacteria. *Mater. Sci. Eng. C.* **2017**, *79*, 270-279, http://dx.doi.org/10.1016/j.msec.2017.05.052.
41. Corrêa, T.H.A.; Holanda, J.N.F. Calcium pyrophosphate powder derived from avian eggshell waste. *Cerâmica* **2016**, *62*, 278–280, http://dx.doi.org/10.1590/0366-69132016623631986.
42. Shavandi, A.A.; Bekhit, A.E.D.; Ali, A.; Sun, Z.; Ratnayake, J.T. Microwave-assisted synthesis of high purity β-tricalcium phosphate crystalline powder from the waste of Green mussel shells (Perna canaliculus). *Powder Technol.* **2015**, *273*, 33–39. https://doi.org/doi:10.1016/j.powtec.2014.12.029.
43. Salimi, E.;Javadpour, J. Synthesis and characterization of nanoporous monetite which can be applicable for drug carrier. *J. Nanomater.* **2012**, *2012*, 1–5, https://doi.org/doi:10.1155/2012/931492.
44. Ruiz-Aguilar, C.; Olivares-Pinto, U.; Aguilar-Reyes, E.A.; Lopez-Juarez, R.; Alfonso, I. Characterization of tricalcium phosphate powders synthesized by sol–gel and mechanosynthesis. *BOL SOC ESP CERAM V* **2018**, *57*, 213–220, https://doi.org/10.1016/j.bsecv.2018.04.004.
45. Opis, H.; Dinu, C.; Baciut, M.; Baciut, G.; Mitre, I.; Crisan, B.; Armencea, G.; Prodan, D.A.; Bran, S. Review: The influence of eggshell on bone regeneration in preclinical in vivo studies. *Biology* **2020**, *9*, 1–17, https://doi.org/10.3390/biology9120476.
46. Rahim, T.A.; Misran, F.; Mustafa, Z.; Shamsudin, Z. Eggshell derived calcium phosphate and its conversion to dense bodies. *ARFMTS* **2020**, *65*, 334–341, http://www.akademiabaru.com/doc/ARFMTSV65_N2_P334_341.pdf.